Supplementary Data for: "Genomic and metabolomic polymorphism among experimentally selected paromomycin-resistant *Leishmania donovani* using clinical isolates from Nepalese patients."

Excel spreadsheets

S1. Results of Principal Component analysis

Principal component analysis (PCA) based on the 219 identified metabolites was generated in order to visualise the major metabolomic differences between each WT and its PMM-R counterpart, and as a quality control check to show that replicated cluster together (Fig. S1). The clones of each isolate were clustered tightly, indicating that variation within each sample was low and results were reproducible. The first (29.6%) and second (24.3%) principal components clustered Sb-S WT, Sb-S PMM-R and Sb-R PMM-R together. principal components clustered Sb-S WT, Sb-S PMM-R and Sb-R PMM-R together, away from the Sb-I WT and the Sb-R WT.

S2. Genetic studies

The sole deletion was in both Sb-S PMM-R isolates as a heterozygous loss of a 1,532 bp region (chr34:1,436,763-1,438,295) containing a NAD-dependent epimerase/dehydratase family gene (LdBPK_340038800, LdBPK_342970) whose *L. major* ortholog POMP27 (LmjF.34.3190) was predicted to have two transmembrane domains and to be located at the outer mitochondrion membrane. This chromosome was disomic for all Sb-S samples. This deletion was likely a product of homologous recombination at flanking repeats (Figure S1): the repeat at bases 1,434,137-534 (398 bases) had 100% identity with that homologous region in *L. infantum* JPCM5 and 88% in *L. major* Friedlin.

A transient duplication of the ribosomal RNA (rRNA) locus on chromosome 27 was discovered in both Sb-S and Sb-R isolates at 2, 4 and 8 μM PMM that was absent in the WT and 32/64/97 μM PMM lines (Figure S4). This locus spanned bases 1,033,794-1,067,796 at LdBPK_270030110-LdBPK_270030260 and encoded 16 rRNA genes ranging in length from 73 to 2,204 bases. This divided into two amplifications: the first was a duplication spanning the whole region, and the second was a triplication at LdBPK_270030120-140 and LdBPK_270030190-220. This reflected the differing initial copy numbers of these loci at the WT stage, with 3.11 haploid copies for the first versus 5.13 for the second, such that amplification rate was approximately equal for the first (1.67) and second (1.76). This was consistent with a pre-existing duplication of the whole locus to a mean of 3.85 haploid copies, and a second pre-existing 1.55-fold amplification of the LdBPK_270030120-140 and LdBPK_270030190-220 portions (resulting in a mean of 5.82 haploid copies). These were followed by a third single amplification of the whole locus by 1.62- to 1.79-fold at 2 to 8 μM PMM that was subsequently lost at higher PMM concentrations, such that the locus returned to a duplication with the amplification of LdBPK_270030120-140 and LdBPK_270030190-220 to three diploid copies. Notably this means the two identical 18S SSU gene copies (LdBPK_270030120, LdBPK_270030190) had gene copy numbers elevated to 5.82 each (11.64 if pooled), compared to the two copies expected.

Table S1 The effect of PMM selection on the metabolic profile of PMM-R *L. donovani* promastigotes compared to WT. The metabolites shown were significantly different ($p < 0.05$) and had a three-fold difference in abundance in one or more of the PMM-R clones compared to its corresponding WT. The table also shows comparisons of the wild type strains. Dats for these sampes is also shown in excel sheet 1 (All data Ldonovani PMMR LCMS.xls)

Pathway	Metabolite	Sb-S (PMMR / WT)	Sb-I (PMMR / WT)	Sb-R (PMMR / WT)	Sb-I/ Sb-S (WT/ WT)	Sb-R / Sb-S (WT / WT)
Amino Acid Metabolism						
Alanine and aspartate	O-Acetylcarnitine	1.07	3.06	1.10	0.77	0.76
Aminophosphonate	Hydroxymethylphosphonate	0.76	2.10	0.24	0.28	1.19
Arginine and proline	(S)-1-Pyrroline-5-carboxylate	1.26	4.02	0.33	1.22	2.79
	4-Guanidinobutanal	1.61	1.01	8.81	0.31	0.16
	4-Guanidinobutanoate	1.04	7.70	0.52	0.73	1.42
	5-Guanidino-2-oxopentanoate	0.47	9.42	0.12	1.16	6.30
	Arginic Acid	1.56	0.85	8.43	0.37	0.16
	Creatinine	1.01	2.53	0.80	0.58	0.78
	L-erythro-4-Hydroxyglutamate	1.79	3.47	0.27	0.82	2.94
	L-Glutamate 5-semialdehyde	0.35	1.56	1.19	0.69	0.38
	L-Ornithine	1.08	0.97	2.33	0.27	0.36
	L-Proline	0.86	3.55	0.64	1.72	1.25
	N-(L-Arginino)succinate	1.44	5.16	0.46	0.12	3.51
	N2-Succinyl-L-arginine	1.01	4.33	0.38	0.40	1.53
	N2-Succinyl-L-ornithine	1.00	2.15	0.22	0.82	3.52
Cyanoamino acid	gamma-Glutamyl-beta-cyanoalanine	0.78	2.52	0.13	0.69	4.34
D-Arginine and D-Ornithine	(2R,4S)-2,4-Diaminopentanoate	0.88	3.05	0.64	0.68	0.94
Glutamate	(R)-2-Hydroxyglutarate	0.75	2.28	0.36	0.23	1.56
Glycine, Serine and	Betaine	0.44	1.88	1.54	0.73	0.29
Threonine	Ethanolamine phosphate	1.38	1.87	0.25	0.58	2.07
	L-2-Amino-3-oxobutanoic acid	2.12	0.98	0.30	0.52	2.62
Glycine, Serine and	L-Serine	0.82	1.29	3.71	1.58	0.25

Threonine.	L-Threonine	0.78	1.39	17.56	1.37	0.06
Histidine	4-Imidazolone-5-propanoate	1.22	1.95	1.63	0.34	0.51
	Imidazol-5-yl-pyruvate	0.37	7.77	0.17	0.57	1.58
	Imidazole-4-acetaldehyde	1.17	1.83	1.79	0.34	0.46
	L-Histidine	0.22	1.70	0.34	0.57	0.84
	N-Carbamyl-L-glutamate	0.85	2.30	0.19	0.75	3.89
Lysine	2,3,4,5-Tetrahydropyridine-2-carboxylate	0.36	1.34	0.95	0.42	0.38
	5-Acetamidopentanoate	2.22	3.87	0.15	1.30	6.10
	6-Acetamido-2-oxohexanoate	1.25	7.87	0.60	1.04	1.39
	L-2-Aminoadipate	0.92	1.50	4.11	0.92	0.15
	L-Carnitine	1.68	2.05	3.79	0.56	0.41
Methionine and cysteine	1-Aminocyclopropane-1-carboxylate	0.32	2.07	1.18	0.43	0.33
	Glutathione	0.60	1.04	21.20	0.56	0.03
	L-Cystathionine	0.26	2.45	2.30	0.63	0.22
	L-Homocysteine	0.15	1.14	0.25	1.15	1.28
	L-Methionine	0.99	1.22	2.94	2.59	0.33
	L-Methionine S-oxide	1.02	6.07	0.94	1.38	0.77
	S-Adenosyl-L-homocysteine	0.35	2.76	0.30	0.24	1.60
Phenylalanine	2-Phenylacetamide	0.69	1.19	0.25	1.63	1.84
	Hippurate	0.30	5.84	1.19	0.84	0.26
	L-Phenylalanine	0.57	1.80	0.16	1.09	2.42
Tryptophan	L-Tryptophan	0.54	2.52	0.16	1.13	2.74
Tyrosine	3-(2-Hydroxyphenyl)propanoate	6.55	0.27	4.14	2.13	0.34
	3-(3-Hydroxy-phenyl)-propanoic acid	3.01	0.57	9.95	0.94	0.17
	3-(4-Hydroxyphenyl)lactate	1.26	5.80	0.21	1.35	3.13
	3-(4-Hydroxyphenyl)lactate	2.04	0.78	5.74	0.78	0.21
	4-Hydroxyphenylacetylglutamic acid	0.48	2.76	0.76	0.34	0.53
	L-Tyrosine	0.62	1.24	0.27	1.46	1.72
Valine, Leucine and Isoleucine	(S)-3-Methyl-2-oxopentanoic acid (KMVA)	1.74	4.58	0.29	1.80	2.83

Carbohydrate Metabolism						
Ascorbate and aldurate	2,3,4-trihydroxy-butanoic acid	1.13	4.92	0.71	1.11	0.95
Butanoate	2-Acetolactate	2.03	3.06	0.28	2.06	4.37
	Diacetyl	2.77	2.81	0.26	3.10	6.23
Carbohydrate	Cellopentaose	0.87	0.37	0.93	0.14	0.67
	Maltotriose	0.84	3.19	0.70	0.69	0.76
	Sucrose	0.37	8.48	0.80	0.51	0.39
Glycolysis / Gluconeogenesis	2-(alpha-Hydroxyethyl)thiamine diphosphate	1.17	3.05	0.62	0.43	1.01
	Pyruvate	1.30	3.86	0.71	0.82	1.23
Pentose and glucuronate	GDP-mannose	0.57	4.94	0.57	0.42	1.14
	UDP-N-acetyl-D-glucosamine	0.88	2.71	0.53	0.29	1.01
	Alpha, alpha'- Trehalose 6-phosphate	1.24	3.30	0.93	0.53	0.94
Pentose phosphate	Deoxyribose	1.57	2.79	3.36	0.30	0.33
	D-Sedoheptulose 7-phosphate	0.97	3.18	1.00	0.32	0.55
	D-Xylulose 5-phosphate	1.03	0.42	1.96	2.26	0.50
TCA cycle	2-Oxoglutarate	0.80	5.97	0.77	0.42	0.72
	CoA	0.81	1.26	9.33	0.68	0.07
Energy metabolism						
	NADPH	0.99	2.91	3.03	0.57	0.48
Cofactors and vitamins						
	5-Methyltetrahydrofolate	0.61	1.16	0.18	0.32	1.66
	8-Amino-7-oxononanoate	2.21	2.65	0.11	2.58	8.04
	Porphobilinogen	0.90	2.28	0.13	0.79	3.19
	Thiamin	0.56	1.75	0.79	0.31	0.46
	Thiamin monophosphate	0.54	2.54	1.07	0.31	0.45
Nucleotide metabolism						
Purine	Adenine	0.98	0.54	0.05	0.44	4.28
	Adenosine	1.00	0.92	0.06	0.23	3.33

	Allantoin	0.84	3.86	0.60	0.41	1.11
Pyrimidine	Thymine	0.84	6.46	0.27	0.63	2.04
No Known Pathway						
	8-Oxodeoxycoformycin	1.42	2.45	0.80	0.25	0.81
	Deoxycytidine	0.42	1.35	0.80	0.26	0.55
	N-[(1R)-1-carboxyethyl]-L-norvaline	3.71	3.39	3.80	1.15	0.52
	(R)-Mevalonate	0.26	1.42	1.77	0.10	0.03
	Capryloylglycine	1.76	4.25	0.15	1.99	7.69
	Iminodiacetate	2.01	0.70	20.00	0.16	0.07
	Linimarin	0.86	2.47	0.31	0.42	1,42
	Muramic acid	1.10	3.40	0.56	0.61	1.40
	N-acetyl-(L)-arginine	1.38	2.32	0.21	0.93	3.52
	N-Heptanoylglycine	2.28	1.23	0.28	4.20	5.37
	p-aminobenzoyl glutamate	1.15	1.51	0.08	0.61	6.77
	Phosphonate	1.85	2.23	1.27	1.04	1.53
	Suberylglycine	1.16	1.17	0.22	1.51	2.76

Table S2 Global effect of PMM selection on the metabolites of PMM-R *L. donovani* promastigotes compared to WT. The overall number of metabolites that had a difference in peak intensity of ≥ 3-fold ($P \leq 0.05$) or ≥ 2-fold ($P \leq 0.05$) increase or decrease.

Comparison	Total Metabolites	≥ 3-fold Increase	≥ 3-fold Decrease	≥ 2-fold Increase	≥ 2-fold Decrease
Sb-S (PMM-R / WT)	214	1	7	9	17
Sb-I (PMM-R / WT)	214	31	1	71	2
Sb-R (PMM-R / WT)	214	13	29	18	50
Sb-I (WT) / Sb-S (WT)	214	2	15	4	19
Sb-R (WT) / Sb-S (WT)	214	12	16	23	23

Table S3. The effect of PMM selection on the lipid profile of PMM-R *L. donovani* promastigotes compared to WT. Lipids that were significantly up regulated (>2.0 fold) are coloured red, down regulated lipids (< 2.0 fold) are coloured blue ($p < 0.05$ comparing PMM-R and corresponding WT.

	Sb-S PMM-R/Sb-S WT	Sb-I PMM-R/Sb-I WT	Sb-R PMM-R/Sb-R WT
Lipids	PI(O-16:0/18:2)		Sphingenine
	PI(O-16:0/20:2)		Cer(d18:0/17:0)
	PI(O-18:0/17:2)		LysoPE(0:0/18:2)
	PI(O-16:0/19:1)		PE (16:0)
	Eicosanoyl-sphingenine		PE (18:1/18:1)
	Hexadecasphinganine		PE(O-20:0/17:2)
	Palmitoyl methionine		PE(P-18:0/17:2)
	Sphinganine		PI(O-16:0/20:1)
Others	Beta-aspartyl-threonine	Sinapyl alcohol	
	Dodecanoic acid	Heptaprenyl-hydroxybenzoate	
		Octaprenyl-hydroxybenzoate	

Table S4 Identification of genomic DNA sequenced on Illumina Hiseq 2000 platforms, with a median sequence coverage of 47.4 ± 17.8 reads per site averaged across 15 sequence libraries. Raw sequence reads are available from the European Nucleotide Archive (ENA) via accession number number ERP115194 and individual sample accession numbers are listed below.

Run_lane_tag	Short Sanger ID	PMM (μM)	Passages	Median Read Depth	Sanger ID	Accession Number ENA
9233_1#16	BPK282P60_1	97	R76(53)	35.6	MHOM/NP/2003/BPK282/0 clone4_SC_60PAR_subclone3 BPK 282/0 clone 4_SC_60PAR_subclone3	ERS197378
8331_7#9	BPK282P60	97	R69(46)	63.2	MHOM/NP/2003/BPK282/0 clone4_SC_60PAR_subclone3 BPK 282/0 clone 4_SC_60PAR_subclone3	ERS161532
8331_8#9	BPK282A1Pc	8	R44(21)	62.3	MHOM/NP/2003/BPK282/0 clone4_SCPAR5 BPK 282/0 clone 4_SC PAR5	ERS160178
8331_8#8	BPK282A1Pb	4	R43(20)	65.2	MHOM/NP/2003/BPK282/0 clone4_SCPAR2.5 BPK 282/0 clone 4_SC PAR2.5	ERS160177
8331_8#7	BPK282A1Pa	2	R43(20)	65.2	MHOM/NP/2003/BPK282/0 clone4_SCPAR1.25 BPK 282/0 clone 4_SC PAR1.25	ERS160176
9233_1#10	BPK282A1_1	0	R34(13)	67.5	MHOM/NP/2003/BPK282/0 clone4 BPK 282/0 clone 4	ERS197372
10747_4#11	BPK275P60_2	97	R76 (44)	32.5	MHOM/NP/2002/BPK275/0 clone18_SC_60PAR_PARENT2 BPK 275/0 clone 18_SC60PAR	ERS340112
10747_4#10	BPK275Pf_1	64	R74 (42)	45.6	MHOM/NP/2002/BPK275/0 clone18_SC_40PAR BPK 275/0 clone 18_SC40PAR	ERS340111
10747_4#9	BPK275Pe_1	32	R58(37)	20.5	MHOM/NP/2002/BPK275/0 clone18_SC_20PAR BPK 275/0 clone 18_SC20PAR	ERS340110
8282_8#9	BPK275A1Pc	8	R55 (24)	40.1	MHOM/NP/2003/BPK275/0 clone 18_SCPAR5 BPK 275/0 clone 18_SC PAR5	ERS197378
8282_8#8	BPK275A1Pb	4	R54 (23)	39.6	MHOM/NP/2003/BPK275/0 clone 18_SCPAR2.5 BPK 275/0 clone 18_SC PAR2.5	ERS161532
8282_8#7	BPK275A1Pa	2	R53 (22)	54.5	MHOM/NP/2003/BPK275/0 clone 18_SCPAR1.25 BPK 275/0 clone 18_SC PAR1.25	ERS160178
10747_4#8	BPK275A1_4	0	R73(52)	25.5	MHOM/NP/2002/BPK275/0 clone18 BPK 275/0 clone 18	ERS160177
9233_1#9	BPK275A1_3	0	R73(52)	22.5	MHOM/NP/2002/BPK275/0 clone18 BPK 275/0 clone 18	ERS160176
8331_7#3	BPK275A1_2	0	R73(52)	71.9	MHOM/NP/2002/BPK275/0 clone18 BPK 275/0 clone 18	ERS197372

Figure. S1 A comparison of glucose metabolism in WT and their corresponding PMM-R strains. **Figure 5. A comparison of glucose metabolism in WT and their corresponding PMM-R strains**. Map of glycolysis, citric acid cycle and the pentose phosphate pathway. Boxed metabolites were detected in metabolic profile of the *L. donovani* strains by LC-MS: yellow shading indicates that metabolite identities confirmed by matching retention times with those obtained with authentic standards, unshaded metabolites were putatively identified by accurate mass only. Unboxed metabolites were not detected by LC-MS but are presumed to be present. Abbreviations: Glucose-6P, Glucose 6-phoshate; Fructose-6P, Fructose 6-phosphate, Fructose-1,6-BP, Fructose 1,6-bisphosphate; GADP, Glyceraldehyde 3-phosphate; PEP, phosphoenolpyruvate; 6P-Gluconate, 6-phosphogluconate; Ribulose-5P, Ribulose 5-phophate; Ribose-5P, Ribose 5-phosphate; Xylulose-5P, Xylulose 5-Phosphate; Sedaheptulose-7P, Sedaheptulose 7-phosphate; Erythrose-4P, Erythrose 4-phosphate.

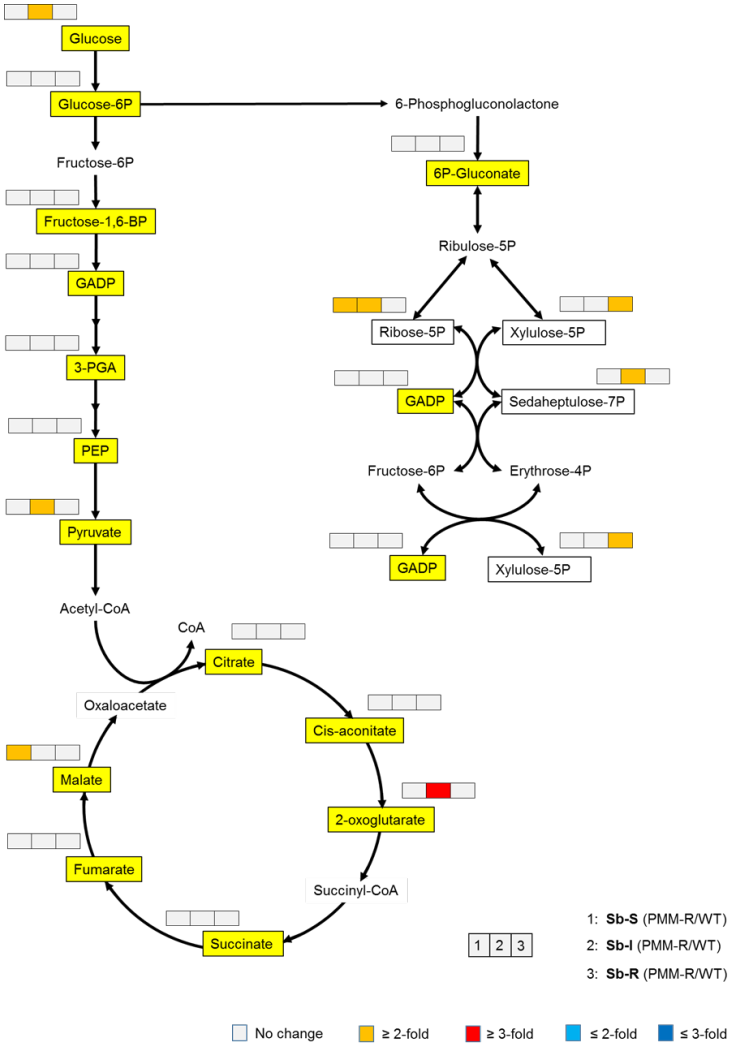

Figure S2. The effect of PMM-R on the genome of Sb-S (BPK282) strain of *L. donovani*. A heterozygous deletion at a NAD-dependent epimerase/dehydratase family gene (LdBPK_340038800) at chr34:1,436,763-1,438,295. The depths of Sb-S WT (bottom) PMM-R (top) are in dark grey. The CDSs are shown as oranges boxes. The y-axis shows the normalised read depth (2 for disomy) as indicated by the dashed red lines. Chromosome 34 was disomic for all samples. BLAST matches show regions of high homology with the red lines. The 398 bases on forward strand at 1434137-534 are: gccacacctcaccgtgcgcggcatctcagggtccagtgcacttccccacccctccccccccgcacaaacacacacacacattatgtctgtgtg cggaggagcgaagcggccccttccaccccacccccccacccccctacctctgctaatgccgaactacctccggccgtgacaagatccagtacc cacagcgtagggatgtcagtgcgatgtatcgctgctgacgccggcggtgtagtcgtggatgggcgcggctgtgatgcgaccagcgaggcact ggtgggtagggtttgaggcaaaggccacgctctccgatggccgggtcggcgcactgctgcaaggcgcgtctgtgcgactgcttcgcacgcac gcgacgtgcccgctgtggcagccccgggggg.

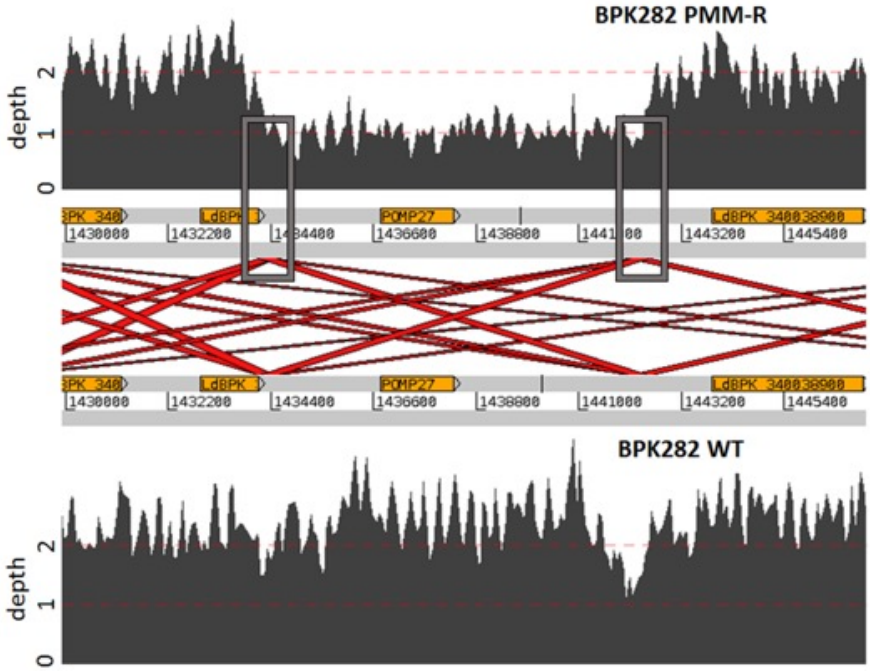

Figure S3. Normalised rRNA haploid gene copy number at the region spanning 1.04-1.08 Mb on chromosome 27 for Sb-S (left) and Sb-R (right). Top: Normalised depth during PMM exposure, which showed two distinct copy number profiles for the rRNA genes. The first had a higher copy number (beige) and spanned two regions encompassing three (LdBPK_270030120-0140) and four (LdBPK_270030190-0220) genes. The second had a lower copy number (pink) and spanned two regions encompassing four (LdBPK_270030150-0180) and four (LdBPK_270030230-0260) genes. Bottom: Normalised depth across the rRNA gene region showed increased copy number at 8 μM PMM (green) for both Sb-S (left) and Sb-R (right) that was absent at 0 μM (mauve) and 97 μM PMM (cyan). The rRNA gene models are shown by the black boxes. LdBPK_270030120-0140 encodes genes for 18S RNA, 5.8S RNA and 28S LSU-alpha (respectively). LdBPK_270030150-0180 encodes genes for 28S LSU-beta, 28S LSU-delta, 28S LSU-zeta and 28S LSU-epsilon M4 (respectively). LdBPK_270030190-0220 encodes genes for 18S SSU, 5.8S M3, 28S LSU-alpha and 28S LSU-gamma M1 (respectively). LdBPK_270030230-0260 encodes genes for 28S LSU-beta, 28S LSU-delta M2, 28S LSU-zeta M6 and 28S LSU-epsilon M4 (respectively). Excel file 2 - Excel file 2 CNV_PPM_BPK282_BPK275_2019.xlsx shows the raw data for rRNA haploid gene copy number used in this figure.